

RESEARCH ARTICLE

CART Based Wide Area Damping Controller Using Global Inter-Area Signal From WAMS

SOHEIL RANJBAR 

Department of Electrical Engineering, Velayat University, Iranshahr 99111-31311, Iran

e-mail: s.ranjbar@velayat.ac.ir

ABSTRACT This paper presents an online scheme of intelligent wide area damping controller based on decision tree (DT) technique using wide area measuring system. In this case, a central damping controller is developed which uses the speed and angle deviations of the oscillating areas as global signals. For this issue, the proposed DT scheme plays as an online gain estimator estimates the controlling gains for direct presentation to exciter systems. The proposed intelligent controller is a non-model and online scheme which plays as global power system stabilizer through real-time environment. In the case of optimizing global controlling signals, considering a set of unstable inter-area oscillations, the proposed DTs are trained off-line which by using inter-area signals in working mode, online controlling gains are estimated. The effectiveness of the proposed control scheme is carried out in the modified IEEE 39-bus test system with indicating positive effects for damping inter-area oscillations.

INDEX TERMS Inter-area oscillations, WAMS, inter-area signal, center-of-inertia, controlling signal, wide area damping controller, power system stabilizer, decision tree CART technique.

ABBREVIATIONS


AI	Artificial Intelligent.	PVG	Photovoltaic Generator.
ANN	Artificial Neural Network.	RBF	Radial Basis Function.
BGA	Binary Genetic Algorithm.	RD	Random Decrement.
CART	Classification and Regression Tree.	RGA	Relative Gain Array.
CC	Correlation Coefficient.	SG	Synchronous Generator.
COI	Center Of Inertia.	SVM	Support Vector Machine.
DT	Decision Tree.	WAMS	Wide Area Measurement System.
FACTS	Flexible AC Transmission System.	WADC	Wide Area Damping Controller.
GCS	Global Controlling Signal.		
GIS	Global Inter-area Signal.		
GPSS	Global Power System Stabilizer.		
GSMIB	Generalized Single Machine Infinite Bus.		
IAO	Inter-Area Oscillations.		
IDI	Inter-area Damping Index.		
LFO	Low Frequency Oscillation.		
LL	Load Level.		
OF	Objective Function.		
OOS	Out-Of-Step.		
PMU	Phasor Measurement Unit.		

I. INTRODUCTION

The IAOs of large power systems are one of LFO types which occurred into the frequency ranges 0.1~1 Hz generally in which there are two oscillating areas consisting of coherent generator groups oscillating each other. In this case, IAOs with weak or negative damping ratio can be attended as a considerable threat for beginning of large blackouts into the system.

A. PAPER MOTIVATIONS

An unstable IAOs are resulted in OOS condition for two oscillating areas which led to separate the power system

The associate editor coordinating the review of this manuscript and approving it for publication was Nagesh Prabhu .

through different uncontrolled islands. Hence, online evaluation of IAOs is an essential necessity for avoiding large-scale blackouts into power systems [1]. Based on the inter-area frequency and its formation, the IAO damping mechanism is different from local oscillation which by using local signals, it is not possible to obtain proper damping performance. Therefore, controlling the IAO damping performances remains as an important issue through power system dynamic security [2].

B. LITERATURE REVIEWS

Over the past two decades, there are several techniques have been concentrated through damping IAOs which can be classified into four different areas including 1-Designing PSS blocks [3], [4], [5], [6], [7], [8], [9], [10], 2-Designing GPSS [11], [12], [13], [14], 3-Identifying controlling signals [15], [16], [17], [18], [19], [20], [21], [22], [23], [24], [25], [26], and 4-Evaluating time latencies through global signals [27], [28], [29].

Based on the developed areas, the first one is concentrated to design PSS block diagrams. In [3], by using approximate decomposition scheme a controlling signal is developed for the PSS feedback signal. In [4], based on developing H_∞ -based technique, a decentralized PSS block diagram is provided. In [5], frequency response method is used for PSS tuning. In [6], by proposing dead-band structure, an adaptive wide area PSS is developed. In [7], a modal decomposition-based scheme is presented for PSS design which by removing the local mode interactions, the PSS performances are evaluated. In [8] and [9], based on evaluating the system mode analysis, an Eigen-value-based index is developed which the PSS parameters are adjusted. In [10], a conic programming-based algorithm is developed for designing both PSS and FACTS damping controllers with each other.

Designing the GPSS controller is the second area in the field of damping IAO which is attended by power engineers. In [11], for designing GPSS, a deviation-error vector is presented for developing dynamic feedback signal which through global error consideration, the corresponding GPSS is designed. In [12], based on developing WAMS structure through real-time environment, a GPSS is presented which by using wide area signals the inter-area modes are controlled. In [13], by using a collocated controlling structure achieved from WAMS data, a systematic procedure of designing GPSS is presented. In [14], by using a GA-based optimization algorithm, the GPSS controlling parameters is evaluated optimally.

Identifying proper controlling signals is the third research activity which is taken into consideration by power engineers. In [15], by using H_∞ loop-shaping technique, the GPSS global signals are developed. In [16] the generators bus voltage magnitudes are proposed to use as additional controlling signal for damping IAO through damping controllers as PSS and FACTS devices. In [17], the tie-line active power and speed deviations are used as input to damping controller for

controlling both local and inter-area modes. In [18], based on developing signal coherency application, a global controlling signal is proposed. Two residue and geometric approaches are presented in [19] for identifying the global signals. In [20], based on the concept of virtual generator (VG), power system is simplified through two inter-area models which by using the VGs signals into COI frame, the corresponding global signals are provided. In [21], a trajectory-based approach is proposed to provide the corresponding global controlling signals. The concept of modal residue minimum variance is used in [22] for identifying the global controlling signals. In the case of developing intelligent schemes, a decision tree-based classification algorithm is proposed in [23] which proper controlling signals are identified. In [24], the concept of observability technique is developed through power system inter-area mode which signals with the most observabilities are selected as the global controlling signals. In [25], based on developing the residue analysis concept, two controllability/observability indexes are developed which the RGA analysis is performed to evaluate proper global signals. In [26], a CART-based decision tree (DT) identification scheme is proposed to estimate proper controlling signals which the corresponding adaptive damping controller is developed.

C. PREVIOUS RESEARCH GAPS

From literature reviews it is resulted that the local signals equipped with damping controllers are not proper way to damp the IAO which a wide area scheme consisting of global controlling signals should be developed. Also, most of the presented methods have been concentrated to damp one severe inter-area mode through identified eigenvalues. In this case, by changing the system operational/ topological conditions, the proposed schemes will not present proper damping performance.

D. PAPER CONTRIBUTIONS

Based on evaluated issues and in order to fill the gaps of previous works, the paper contributions and main novelties are proposed through following items:

- i) Proposing a generalized approach of presented WADC scheme [2] based on developing centralized WADC instead of distributed scheme [2] for damping the IAOs.
- ii) Evaluating the effects of time delay on WADC damping performance.
- iii) Developing the decision tree technique through two centralized CART1 and CART2 technique for estimating the optimal gains of centralized WADC controller.
- iv) Proposing an IDI index to find the most effective WADC schemes.

Based on developed novelties, an intelligent CART-based WADC strategy is presented in this paper which is concentrated for damping IAOs through large power systems equipped with WAMS technologies. For this issue, a central damping controller is proposed which utilizes the speed and angle deviations ($\Delta\omega_{COI}$, $\Delta\delta_{COI}$) of two oscillating areas provided in COI frame as GISs and present the corresponding

GCSs for direct presentation to the generators exciter systems. The proposed intelligent WADC scheme plays as a GPSS which provide proper GCSs through generator AVR with positive effects on the damping performances. It should be noting that, the installed local PSSs are tuned to damp the individual local oscillations without any actions through damping the IAO. The proposed WADC scheme is a non-model based and online controller consists of two CARTs estimators for estimating the GIS controlling gains through real-time working mode. In the case of training CARTs, considering a set of unstable IAOs, two developed CARTs are trained offline which by using GIS signals through real-time working mode, proper controlling gains are estimated.

E. PAPER ORGANIZATIONS

This paper is organized as follows:

In *Sec.II*, conceptual model of the inter-area oscillation is developed. In *Sec.III*, the mechanism and nature of IAO damping power is presented. The conceptual and detailed structures of the proposed WADC scheme is presented in *Sec.IV*. In *Sec.V* the time domain simulations and numerical results are presented while the related conclusion will be discussed in *Sec.VI*.

II. THE MODEL OF INTER-AREA OSCILLATIONS

IAO is a specific type of LFOs in power system which there are two or more coherent areas oscillating with respect to each other. Actually, the main requirements for developing IAOs in power systems can be summarized within two following points including (a) Forming a set of synchronous generator within different coherent groups and (b) Forming IAO between coherent groups with rotor angle phase difference more than 90 degrees through negative damping ratio. In the case of identifying two oscillating areas, it is known as an IAO which can be threatred through power system security. For modeling IAO, based on the COI concept, each coherent group can be approximated by a separate VG with individual parameters as follows:

$$\delta_{COI} = \left[\sum_{i=1}^n H_i \times \delta_i \right] / \left[\sum H_i \right] \tag{1}$$

$$\omega_{COI} = \left[\sum_{i=1}^n H_i \times \omega_i \right] / \left[\sum H_i \right] \tag{2}$$

$$H_{COI} = \sum H_i \tag{3}$$

From (1)-(3), δ_i , ω_i and H_i are the generator rotor angle, speed deviation and inertia of the i th synchronous generator, respectively. Also, δ_{COI} , ω_{COI} and H_{COI} are the equivalent rotor angle, speed and the inertia of each individual coherent VG, respectively. By this way, power system can be modeled through two equivalent VGs including VG_A and VG_B oscillating against as shown in Figure 1-a. Based on Figure 1-a, in the case of forming two oscillating areas, the equivalent

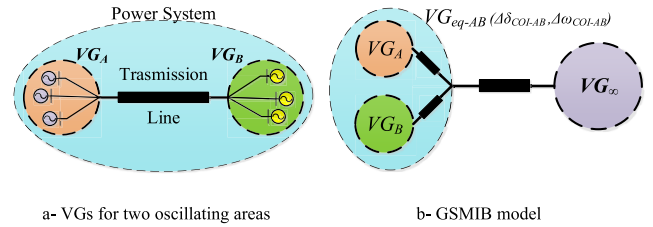


FIGURE 1. Equivalent model for IAOs.

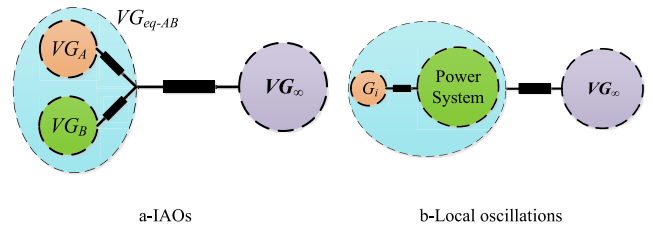


FIGURE 2. GSMIB models for local and IAOs.

COI frame can be regarded as the proposed GIS signals as follows:

$$\Delta\delta_{COI-AB} = \Delta\delta_{COIA} - \Delta\delta_{COIB} \tag{4}$$

$$\Delta\omega_{COI-AB} = \Delta\omega_{COIA} - \Delta\omega_{COIB} \tag{5}$$

From (4) and (5), it should be noted that the basic concept of the well-known SMIB model can be extended in this study for modeling the IAO in the form of two VGs oscillating areas as VG_A and VG_B . In this case, two developed VGs are merged together in the form of new equivalent VG as VG_{eq-AB} which is denoted as the inter-area VG as shown in Figure 2-b. Similar to SMIB concept, the developed VG_{eq-AB} oscillates against an infinite generator (i.e. infinite bus) with two equivalent $\Delta\delta_{COI}$, $\Delta\omega_{COI}$ signals which can be known as GSMIB model for modeling IAOs.

From Figure 1, considering two VGs, the equivalent inertia constant (H_{AB}) of the VG_{eq-AB} model is represented as follows:

$$H_{eq-AB} = [H_{VG_A} \times H_{VG_B}] / [H_{VG_A} + H_{VG_B}] \tag{6}$$

From (6), the constants H_{VG_A} and H_{VG_B} represent the equivalent inertia of two VGs of VG_A and VG_B , respectively. From Figure 1-b, it can be concluded that, by mitigating two VGs within an equivalent model, there is a generalized model VG_{eq-AB} which oscillates against a virtual infinite generator. The provided dynamic signals ($\Delta\delta_{COI-AB}$, $\Delta\omega_{COI-AB}$, H_{COI-AB}), can be evaluated against the infinite equivalent generator VG_∞ as follows:

$$\Delta\delta_{VG_{AB-\infty}} = \Delta\delta_{COI-AB} - \Delta\delta_{VG_\infty} \tag{7}$$

$$\Delta\omega_{VG_{AB-\infty}} = \Delta\omega_{COI-AB} - \Delta\omega_{VG_\infty} \tag{8}$$

$$H_{VG_{AB-\infty}} = [H_{COI-AB} \times H_{VG_\infty}] / [H_{COI-AB} + H_{VG_\infty}] \tag{9}$$

From (7)-(9), $\Delta\delta_{VG_\infty}$, $\Delta\omega_{VG_\infty}$ and H_{VG_∞} represent the rotor angle, speed deviation and inertia constant of the infinite

generator, respectively. Conceptual structure of the developed GSMIB model is shown in Figure 2.

From Figure 2, in the case of local oscillation, GSMIB model is represented as a power system which oscillates against the infinite bus. However, in the case of IAO, there are VGs equaled as one equivalent virtual generator VG_{eq-AB} which oscillate against the infinite generator with corresponding rotor angle, speed and inertia parameters. It should be noting that the proposed GSMIB concept could be extended for all real power systems consisting of different inter-area modes.

It should be noted that the high penetration of inverter-based resources like wind and solar energies can lead to challenges in the Grid as a) Reduction the grid inertia may raise stability and reliability issues, b) Degrading the grid strength and short circuit current levels may cause stability and protection issues, and c) Damping oscillations, providing resonance solutions, and riding through a fault without traditional synchronous generators can be challenging in systems.

Fortunately, the Type 5 wind turbines addressed all these challenges by implementing typical wind turbine generator equipped with variable-speed drive connected to a torque/speed converter coupled with a synchronous generator. In this case, based on the Type 5 wind turbine model and evaluating the wind generator rotor angle and speed deviations, it can be used on proposed inter-area model to provide more actual model of the system IAO.

Moreover, in the case of solar generation, PVG is based on semiconductor device and solid-state synchronous voltage source converter that is analogous to a synchronous machine except the rotating part. The PVG generates sinusoidal voltage at fundamental frequency with rapidly controllable amplitude and phase angle to inject the active and reactive power to the power system. In this case, using the phase angle and angular frequency of PVG buses, it is possible to evaluate the PVG models in the inter-area model. However, due to lacks of PVG inertias, they do not have contributed effectively on inter-area model, the output active powers generated by PVGs present positive impact on damping the inter-area oscillations in power systems. Detailed descriptions of this point can be found in [31] and [32].

III. DAMPING INTER-AREA OSCILLATION

Based on the concept of GSMIB model and PSS damping power, it is deduced that the most proper method for damping the IAOs is to produce a damping power in-phase with the evaluated inter-area speed deviation ($\Delta\omega_{COI-AB}$) as follows:

$$\Delta P_{Damping}^{inter-area} = K_{Damping} \times \Delta\omega_{COI-AB} \quad (10)$$

From (10), it should be noted that the basic concept of producing inter-area damping power is an inter-area GCS which all generators oscillating against each other must participate through its damping performances. This point can be expressed within two different cases including *Case1*-Local signals produced from local PSS and *Case2*-Developing GCSs using GPSSs for providing inter-area damping power.

In *Case1*, local PSSs receive the speed deviation of individual generators which provide an additional damping power in-phase with the local speed oscillations as follows:

$$\Delta P_{Damping-i}^{Area-A} = K_{Di-A} \times \Delta\omega_{i-A} ; \forall i \in Area A \quad (11)$$

$$\Delta P_{Damping-j}^{Area-B} = K_{Dj-B} \times \Delta\omega_{Dj-B} ; \forall j \in Area B \quad (12)$$

From (11) and (12), the produced damping powers are in-phase with the oscillation of each equivalent area which the total damping power of each area achieved from individual damping powers of local PSSs can be evaluated as follows:

$$\begin{aligned} \Delta P_{Damping}^{Area-A} &= \sum \Delta P_{Di-A} = (\sum K_{Di-A}) \times \Delta\omega_{COI-A} \\ &= K_{DA} \times \Delta\omega_{COI-A} \end{aligned} \quad (13)$$

$$\begin{aligned} \Delta P_{Damping}^{Area-B} &= \sum \Delta P_{Dj-B} = (\sum K_{Dj-B}) \times \Delta\omega_{COI-B} \\ &= K_{DB} \times \Delta\omega_{COI-B} \end{aligned} \quad (14)$$

From (13) and (14), it is deduced that the produced damping powers from local PSSs are in-phase with the equivalent speed oscillation of each coherent group ($\Delta\omega_{COI-A}$, $\Delta\omega_{COI-B}$) and not in-phase with the corresponding inter-area speed deviations ($\Delta\omega_{COI-AB}$). Therefore, the produced damping powers have no positive effects through damping the IAO.

In *Case-2*, by using proposed GIS signal, all of installed PSSs receive an inter-area signal from IAOs which provide an individual damping power in-phase with the inter-area speed oscillation. In this case, the total additional damping powers obtained from each coherent area are in-phase with the evaluated inter-area speed deviation ($\Delta\omega_{COI-AB}$) as follows:

$$\begin{aligned} \Delta P_{Damping}^{Area-A} &= (\sum K_{Di-A}) \times \Delta\omega_{COI-AB} \\ &= K_{DA} \times \Delta\omega_{COI-AB} \end{aligned} \quad (15)$$

$$\begin{aligned} \Delta P_{Damping}^{Area-B} &= (\sum K_{Di-B}) \times \Delta\omega_{COI-AB} \\ &= K_{DB} \times \Delta\omega_{COI-AB} \end{aligned} \quad (16)$$

Based on signals (15) and (16), it is possible to present the final additional damping power provided as follows:

$$\begin{aligned} \Delta P_{Damping}^{AB} &= \Delta P_{Damping}^{Area-A} + \Delta P_{Damping}^{Area-B} \\ &= (K_{DA} + K_{DB}) \times \Delta\omega_{COI-AB} \end{aligned} \quad (17)$$

From (17), it is concluded that the damping power is in-phase with the IAO which therefore has positive effect through damping the IAO. Considering two provided cases (*Case-1* and *Case-2*), it can be seen that by using the local signals in *Case-1*, the produced damping power is in phase with the local equivalent areas and do not have effective results through IAOs. However, in *Case-2*, by using inter-area signals, the final produced damping powers are in phase with the identified IAOs and present positive effects. In addition, it is resulted that the most proper controlling signal for damping each type of IAO is a GIS in-phase with the excited inter-area mode.

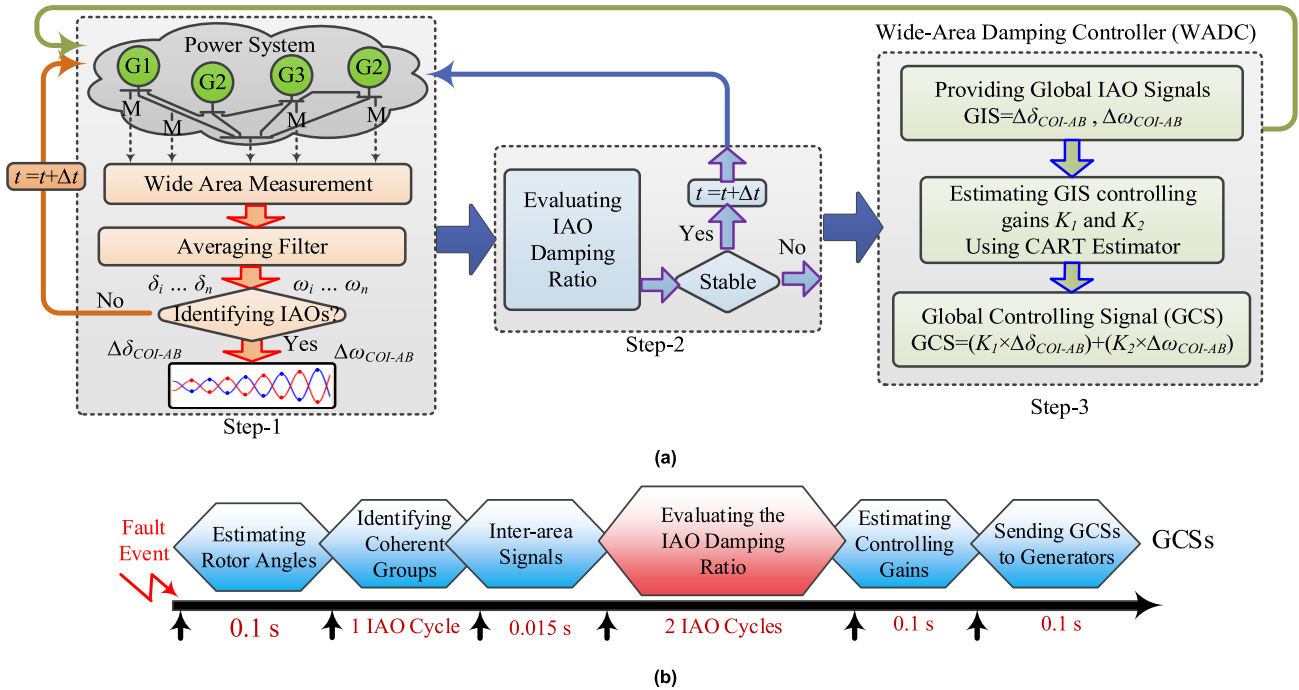


FIGURE 3. Real-time structure of the proposed WADC scheme (a) Real-time procedure, (b) Computation time.

IV. THE PROPOSED WADC SCHEME

The real-time structure and required computation time of the proposed WADC scheme consisting of CART-based decision tree for estimating the GIS controlling gains based on WAMS technology is shown in Figure 3(a) and Figure 3(b), respectively. In real-time working mode, considering each time window (Δt) consisting of inter-area peak points, the system dynamic security is evaluated in which based on phasor signals achieved from WAMS data, the generators dynamic signals (i.e. ω_i and δ_i) are estimated [2]. For online identifications of coherent groups, based on the concept of correlation coefficient and by using clustering technique developed in [2], the system dynamic signals are evaluated from which generators with the potentials of forming coherent groups are identified.

By evaluating two or more coherent groups, using the inter-area signals developed in (1-5) and evaluating the inter-area damping ratios against each other, the corresponding oscillating areas are identified. In the case of identifying two oscillating areas with unstable damping ratios, the proposed WADC scheme is activated which performs as a GPSS at the control center for providing proper GCSs to damp the IAOs. It is worth noting that the proposed WADC scheme is an adaptive and online CART-based damping controller which the GCG controlling gains are estimated by using CART-based optimal gain estimator through online working mode. In this case, the produced proper GCSs are presented to the excitation systems of the generators through both identified oscillating areas.

It should be noted that in the case of power systems with multiple inter-area modes, based on online evaluations of the generator dynamic variables ω_i and δ_i , the oscillating areas are identified. In this case, based on identified two oscillating areas, the inter-area speeds and rotor angles are evaluated and used as GISs. Therefore, as it can be seen, based on real-time evaluations, the combinations of the proposed GISs are different which based on excited the inter-area mode, only coherent generators in two oscillating areas are incorporated in developing the WADC inter-area signal.

Time latencies into the WAMS-based communication systems are an essential issue which resulted in improper effects in the WADC applications.

Though literature review, there are many researches which present multiple techniques to compensate the WAMS latencies [3], [4], [7], [12]. However, in this study, the main goal is to provide an intelligent and online WADC controller in which it is considered the unavoidable time delays from WAMS data are compensated by appropriate presented techniques.

Also, based on Figure 3(b), the proposed controller requires two oscillating inter-area cycles for evaluating and estimating controlling signals. The required time computations are included as estimating rotor angle (0.1 s), identifying coherent groups (one inter-area cycle), developing inter-area signals (0.015 s), evaluating inter-area damping ratio (2 inter-area cycles), estimating controlling gains K_1 and K_2 (0.1 s) and sending GCSs to candidate SGs (0.1 s).

Based on the WADC scheme developed in Figure 3, the structures of the presented steps are detailed as follows:

A. INTER-AREA OSCILLATION IDENTIFICATION

In bulk power systems consisting of multiple synchronous generators, the formation and structure of the oscillating areas are depended on the fault locations, the installed damping controllers, the system operational and topological structures. In the case of forming an IAO, the online and accurate identification of possible coherent groups is an emergency issue for determining proper controlling actions. For this issue, at each time window (Δt), based on the WAMS data through online working mode, the generators dynamic signals (i.e. rotor angles and speed deviations) are estimated. Then, based on mathematical formulation (18), the CC parameters within each two pairs (δ_i, δ_j) of synchronous generators are evaluated which generators with the potential of forming into one coherent group are identified.

$$R_{ij} = \frac{n \sum (\delta_i \delta_j) - (\sum \delta_i)(\sum \delta_j)}{\sqrt{[n \sum \delta_i^2 - (\sum \delta_i)^2][n \sum \delta_j^2 - (\sum \delta_j)^2]}} \quad (18)$$

From (18), R_{ij} represents the CC value between the i th and j th generators, respectively. Also, n represents the number of sampling ratio at each time window Δt . Detailed expressions related to presented CC technique are given in [2].

B. EVALUATING INTER-AREA OSCILLATION DAMPING RATIO (IDR)

In the case of identifying an unstable IAO, it is required to evaluate the inter-area damping ratio as an online index to activate the proposed WADC scheme. In this study, at each time window, by using the RD technique [10], GIS signals (4) and (5) are evaluated accurately which the damping ratios of identified IAOs are computed. RD is a simple and averaging-based technique which uses the average values of the inter-area signals. In this case, by using average values of time segments, the inter-area signal is evaluated which average value of damping ratio at each time window is determined. For this propose, considering an inter-area signal $\omega_{COI-AB}(t)$ through N time segments, the signal damping ratio D_{xx} can be evaluated as follows [2]:

$$D_{xx}(\tau) = \frac{1}{N} \sum_{i=1}^N \omega_{COI-AB}(\tau + t_i) |Tx(t_i) \quad (19)$$

From (19), $Tx(t_i)$ represents the DR triggering situation which uses the N numbers of time segments for averaging the inter-area signal. The real-time procedure of proposed RD technique can be developed through following three steps:

Step-1: Initializing time segment triggering.

Step-2: Averaging the signal through evaluated data segments.

Step-3: Evaluating IDR through averaged RD data.

One of the most important advantages of the proposed RD technique is the noise reduction through averaging processes. This point is important because in real-time measurements, the oscillating signals involving with some unavoidable noises which may be resulted in improper performance of damping controllers. In the case of evaluating RD

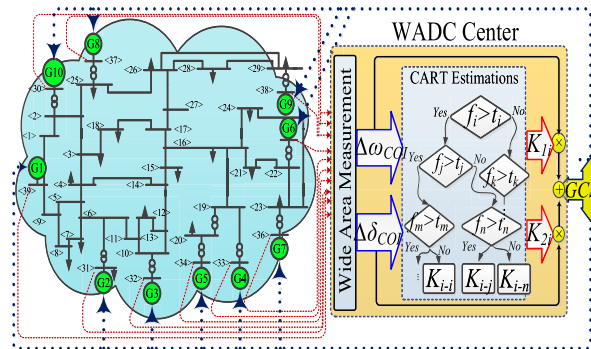


FIGURE 4. Detailed structure of the proposed WADC scheme.

value through GIS signal, considering curve fitting function through averaged values, the GIS damping ratio is estimated.

C. WIDE AREA DAMPING CONTROLLER

By identifying an unstable IAO, the proposed WADC scheme is activated which produces proper GCS for direct presentation to the generators excitation systems. Detailed structure of the proposed WADC scheme us shown in Figure 4.

From Figure 4, by evaluating IAOs, GISs are sent for two optimal gain estimators CART1 and CART2 which proper controlling gains K_1 and K_2 are estimated individually. For this propose, the mentioned GCS of developed WADC scheme can be written as follows:

$$GCS = K_1 \cdot \Delta\omega_{COI-AB} + K_2 \cdot \Delta\delta_{COI-AB} \quad (20)$$

where, $\Delta\omega_{COI-AB}$ and $\Delta\delta_{COI-AB}$ are the inter-area speed and inter-area rotor angle oscillations merged in COI frame.

In the case of estimating two gain factors K_1 and K_2 , it should be noted that inter-area modes have different damping ratios and frequencies which require an adaptive damping controller to present damping power in-phase with the excited inter-are mode. This is the just way which can control an inter-area mode. Therefore, to provide the WADC proper damping powers, K_1 and K_2 present important role which based on identifying the inter-area oscillation frequency and damping ratio, controlling gains should be adapted to present the WADC output power in-phase with the oscillations.

From (20), two estimators CART1 and CART2 are responsible for online estimation of optimal gains K_1 and K_2 through real-time working mode. For this issue, using a set of unstable IAOs in offline mode, two CARTs are trained properly which estimate proper gains of proposed WADC scheme through real-time working mode. It is worth noting that, since, the proposed GCS consists of two GISs (i.e. $\Delta\omega_{COIAB}, \Delta\delta_{COIAB}$) with 90 degrees phase shift differences, so by accurate estimation of two controlling gains K_1 and K_2 , proper damping power with the potential of positive effects through damping IAOs are provided.

It should be noted that the proposed controlling signal GCS (20) equipped with two inter-area signals $\Delta\omega_{COIAB}$ and

$\Delta\delta_{COIAB}$. Since, these two dynamic signals have 90 degrees phase shift differences in natural, so the proposed WADC controller acts as the 1th order transfer function to compensate the inter-area phase shift and present proper the inter-area damping powers. In this case, based on the phase shift requirements, the contributions of $\Delta\omega_{COIAB}$ and $\Delta\delta_{COIAB}$ are different. In this case, each inter-area signal has its own controlling gains K_1 and K_2 , individually. Therefore, based on the system online evaluations, both K_1 and K_2 are contributed in which by accurate estimation of the controlling gains K_1 and K_2 , proper damping power with the potential of positive effects in damping inter-area oscillation are provided.

Also, in order to estimate the controlling gains properly, two different decision tree estimators CART1 and CART2 are required to be trained. In this case, through offline working mode, different topological and operational conditions are evaluated in which scenarios with the potential of exciting inter-area modes are identified. For this purpose, throughout five different load levels, the line outages contingencies with the potential of unstable inter-area oscillations are developed. Then, based on the time domain simulations on offline working mode, and implementing the BGA as optimization engine with the aim of minimizing inter-area oscillations (21), the WADC controlling gains (K_{1i} , K_{2i}) are optimized. In this case, for each scenario, the inter-area oscillations peak points at post-fault durations and optimized individual controlling gains (K_{1i} , K_{2i}) are used as two input-output pairs data and stored in a databox for training the CART1 and CART2. It should be noted that in the case of reaching proper results, two upper and lower criteria $0 < K_1 < 100$ and $0 < K_2 < 100$ are specified as the controlling gains constraints.

Finally, at each time moving window in real-time evaluations, in the case of identifying unstable inter-area oscillations, the proposed WADC two estimators CART1 and CART2 are activated in which based on evaluating the oscillation peak points, proper controlling gains are estimated online.

It is worth noted that, the propose WADC scheme is an intelligent controller based on decision tree technique requires training data for proper online estimations. Therefore, in the case of lack of training data or improper training samples, decision tree cannot be trained very well which the output estimation will be inaccurate.

V. SIMULATION STUDIES

In this section, considering the IEEE-39 bus test system consisting of 10 SGs connected through tie-lines, damping performance of the proposed WADC scheme is evaluated. As it is shown in Figure 5, the installed synchronous generators have a potential of forming two oscillating areas *Area-A* (G1,G2,G3,G4,G5,G6,G7) and *Area-B* (G8,G9,G10) based on the system operational and topological conditions. In this case, in order to control generators dynamics through both local and IAOs, each generator is equipped with two individual controllers including a local PSS for damping the local oscillations and a WADC scheme for damping the

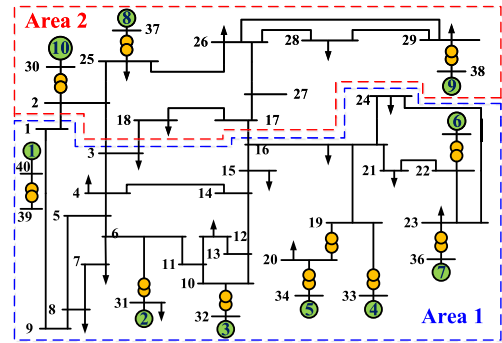


FIGURE 5. IEEE test system with the potential of two oscillating areas.

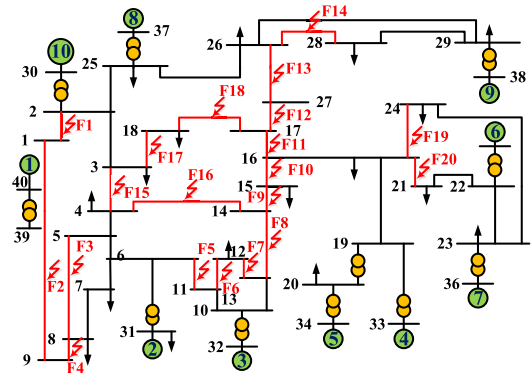


FIGURE 6. Line outages with the potentials of inter-area oscillations.

IAOs. Also, all of generator terminals are equipped with PMU devices which the voltage and current phasor are evaluated and sent to the proposed WADC-based control center synchronously through WAMS-based technology.

It should be noted that all of simulation studies investigated for evaluating and performing the proposed WADC scheme in real-time working mode are carried out by DigSILENT® programming languages which is powerful software for simulating power system dynamic stability.

A. CART-BASED OPTIMAL GAIN ESTIMATOR ORGANIZATION

In order to proper estimation of GCS controlling gains, two individual CART-based estimators are selected which are optimized through following evaluation processes:

- 1) PREPARING THE INTER-AREA OSCILLATION SCENARIOS
For providing proper training data needed for training two intelligent CARTs, considering the topological and operational conditions through offline mode, the inter-area modes are excited. For this purpose, considering five LLs including $LL1=5869$ MW, $LL2=6312$ MW, $LL3=6625$ MW, $LL4=6762$ MW and $LL5=7223$ MW, the system dynamic behaviors are evaluated. In this case, considering single- and two-line outages with the potential of unstable IAOs, system dynamic oscillations are investigated. Figure 6 presents the

corresponding line contingencies with the potential of forming oscillating areas through unstable IAOs.

From Figure 6, for each contingency, considering the time domain simulation studies, the generators rotor angles and speed deviations are evaluated. Finally, considering five load levels through 20 single contingencies, there are 100 unstable scenarios used for CARTs trainings. For each scenario, using the correlation coefficients theory developed in Sec. IV-A, the possible coherent groups are identified the corresponding GIS signals ($\Delta\omega_{COIAB}$, $\Delta\delta_{COIAB}$) are provided.

2) OPTIMIZING THE CONTROLLING GAINS USING BGA ALGORITHM

In this section, required procedures of the optimizing global controlling gains are presented. Through offline mode, considering each oscillating scenario i , by using GISs as input signals and implementing BGA as optimization engine, the WADC optimal controlling gains (K_{1i} , K_{2i}) are computed. For this issue, considering the OF developed in (21) and evaluating the developed IAO with the aim of minimization OF, the corresponding optimization process are carried out which proper individual controlling gains are provided.

$$\min : OF = \int_0^T (\Delta\omega_{COI-AB}).dt \quad (21)$$

From (21), considering 100, 100 and 50 as the initial populations, the iterations and the simulation time duration, respectively, IAOs are investigated. Also, two upper and lower boundaries $0 < K_1 < 100$ and $0 < K_2 < 100$ are specified as the controlling gains constraints. In the case of IAOs, the GIS signals and corresponding individual controlling gains (K_{1i} , K_{2i}) are used as two input-output pairs data for training the CARTs through offline mode. By this way, generators with positive effects on damping IAO specified with higher gain values which generators with low effects associated with lower gain values in optimization processes.

3) TRAINING CART TECHNIQUE

The proposed CART scheme is a DT-based intelligent technique which structures from top to down in a heuristic search presentation. Considering each determined feature (i.e. $\Delta\omega_{COIAB}$, $\Delta\delta_{COIAB}$ in this paper), a set of questions are associated and the training datasets are classified. For this propose, the Gini and Entropy indexes are two well-known parameters which are evaluated for classifying datasets. In this case, through non-leaf nodes, features with the highest Gini indexes are determined and the CART grows through nodes distributions into two individual sub branches.

In this paper, the numbers IAOs peak points which represent the oscillations damping ratios are selected as input data to CARTs. Actually, the corresponding peak point numbers present positive effects through training performance. For this purpose, 10 numbers of peak points of GIS signals ($\Delta\omega_{COIAB}$, $\Delta\delta_{COIAB}$) are selected and used as input to both CART1 and CART2. It should be worth noting that all of the required

TABLE 1. Cart1 training performance through estimating the gain K_1 .

Peak point	Feature1 ($\Delta\omega_{COI-AB}$)		Feature2 ($\Delta\delta_{COI-AB}$)		Feature3 ($\Delta\delta_{COI-AB} + \Delta\omega_{COI-AB}$)	
	Linear Correlation Results					
	Train	Test	Train	Test	Train	Test
1	0.91	0.89	0.9	0.71	0.99	0.92
2	0.99	0.84	0.97	0.64	0.99	0.64
3	0.95	0.93	0.95	0.75	0.97	0.93
4	0.96	0.91	0.99	0.72	0.97	0.9
5	0.98	0.9	0.96	0.46	0.97	0.98
6	0.97	0.93	0.96	0.55	0.95	0.77
7	0.98	0.93	0.99	0.73	0.95	0.77
8	0.99	0.85	0.98	0.64	0.95	0.79
9	0.99	0.85	0.98	0.71	0.95	0.79
10	0.99	0.85	0.98	0.71	0.95	0.79

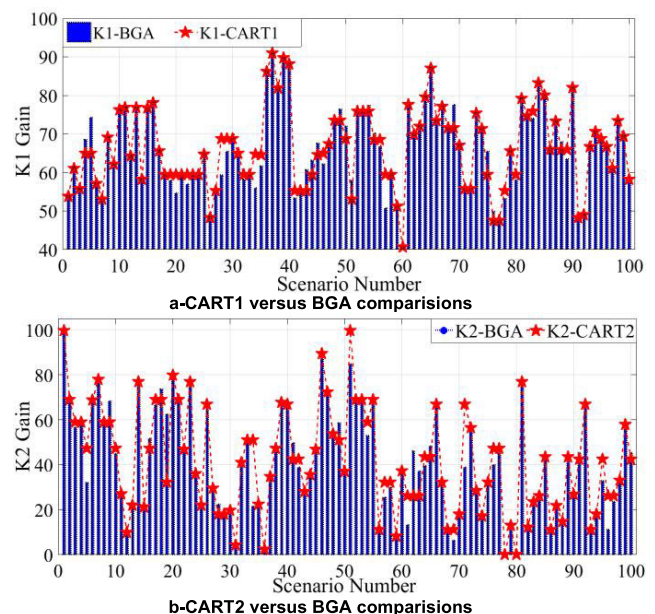


FIGURE 7. CARTs estimated gains compared with BGA optimized values.

DT-based mathematical formulations are developed through MATLAB m-file programming tools which then the proposed CART accuracies are evaluated. Results of CART1 training performance with respect to inter-area peak points are shown in Table 1.

From Table 1, it is indicated that the inter-area peak points have positive effects through CART accuracy which 5 peak points present the highest accuracy between the training and testing values based on the linear correlation evaluation. Also, considering two inter-area signals $\Delta\omega_{COI-AB}$ and $\Delta\delta_{COI-AB}$ both with together represent better accuracy than considering each feature, separately. A comparative analysis through CART-based estimated gains K_1 and K_2 and BGA optimized gains through 100 oscillating scenarios are presented in Figure 7.

4) COMPARISON THE CART SCHEME WITH OTHER AI TECHNIQUES

In order to validate the CART estimation values, considering two AI techniques including SVM and ANN, the CARTs

TABLE 2. Comparing performance of CARTs with ANN and SVM techniques.

Peak point	CARTs	ANN	SVM
	Linear Correlation	Linear Correlation	Linear Correlation
1	0.92	0.47	0.44
2	0.64	0.3	0.44
3	0.93	0.47	0.46
4	0.9	0.45	0.48
5	0.98	0.42	0.56
6	0.77	0.44	0.57
7	0.77	0.51	0.37
8	0.79	0.5	0.36
9	0.79	0.33	0.36
10	0.79	0.43	0.36

estimated values are validated. In this case, by using similar training procedure for both SVM and ANN techniques and considering $\Delta\omega_{COI-AB}$ and $\Delta\delta_{COI-AB}$ peak points as input features, their accuracies are evaluated. In the case of SVM training, its training performance is properly optimized by adjusting the SVM α and η parameters as 0.1 and 0.9, respectively. Also, a kernel type based on RBF technique with the standard deviation 0.1 is used through training processes. In this case, different $RBF\gamma$ values consisting of 0.1,10, and 1000 are evaluated from which the $RBF\gamma = 1000$ indicated the highest accuracy and used through SVM evaluations. For training the ANN technique, considering a multilayer perceptron equipped with 10 neurons through hidden layer and by using feed forward-type neural network with back-propagation training algorithm, the ANN parameters are optimized. In this case, considering 350 training iterations, the ANN training performance reached to optimized value with the highest possible learning accuracy. The estimation performance of CART-based decision tree with two well-optimized SVM and ANN techniques are shown in Table 2. From Table 2, it can be seen that CARTs represent better performances compared with two other techniques through all peak point numbers.

B. CASE STUDIES

In the case of training two CARTs completely, they are performed in real-time working mode which GCS controlling gains are estimated online in real-time working mode. In this case, for evaluating damping performance of the proposed WADC scheme through real-time evaluations, considering two following unstable IAO scenarios have not seen during training processes, the CARTs estimations and corresponding WADC damping performances are evaluated.

1) CASE 1

In the first scenario, considering the load level $LL3=6625$ MW, a 3-phase short circuit fault event is occurred on line 16-17 at $t=2$ second which by implementing the tie-line relay actions, two lines 16-17 and 3-18 are tripped at $t_1 = 2.1$ second and $t_2 = 2.3$ second, respectively. Following with the occurred fault event, the system dynamic response is evaluated. The

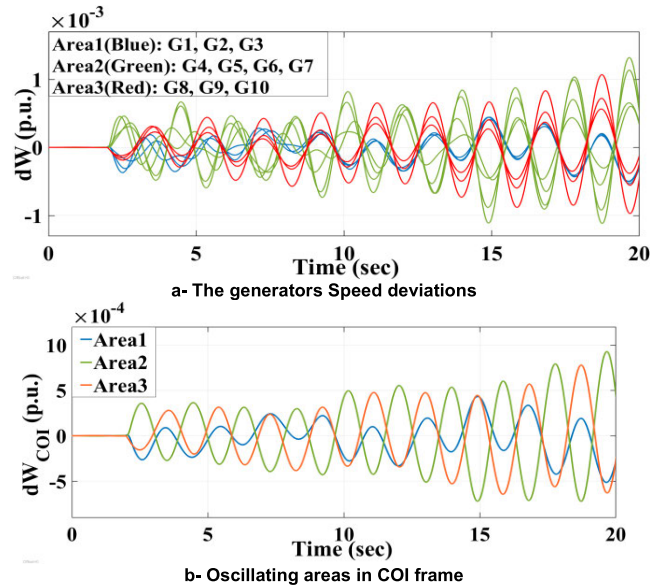


FIGURE 8. IAOs without WADC-Case 1.

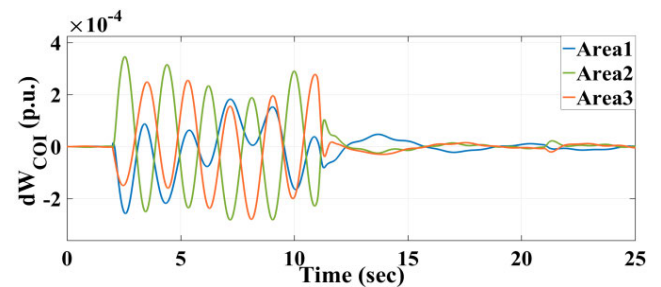


FIGURE 9. IAOs in COI frame with WADC activation-Case 1.

generator speed deviations ($d\omega$) and corresponding oscillating areas are shown in Figure 8-a and Figure 8-b, respectively.

From Figure 8-a, by evaluating the system dynamic behavior and based on the proposed correlation coefficient theory, the system synchronous generators are divided into three generator coherent groups including *Area1*(G1,G2,G3), *Area2*(G4,G5,G6,G7) and *Area3*(G8,G9, G10). In this case, by using the signal formulations (1) and (2), three GIS signals are evaluated which as shown in Figure 8-b. As it is shown, *Area2* is anti-phase against with the *Area3* with the $f=0.57$ Hz inter-area frequency. For this issue, based on the GIS signals (4) and (5), two inter-area signals $\Delta\omega_{COI-2-3}$ and $\Delta\delta_{COI-2-3}$ are determined as input signals to WADCs which by evaluating 5 inter-area peak points, the specific controlling gains K_{1i} and K_{2i} are estimated by two CARTs. The estimated gains of two CARTs are $K_{1-CART1} = 48.65$ and $K_{2-CART2} = 24.86$ which are highly close with the BGA offline results $K_{1-BGA} = 49.14$ and $K_{2-BGA} = 24.25$. In the case of estimating controlling gains, by passing 5 inter-area peak points, the proposed WADC scheme is activated which the GCSs are sent to the mentioned synchronous generators installed into the areas *Area2* and *Area3*. The corresponding

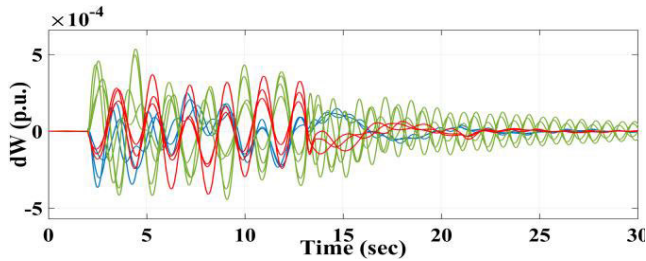


FIGURE 10. WADC damping performances considering time delay-Case 1.

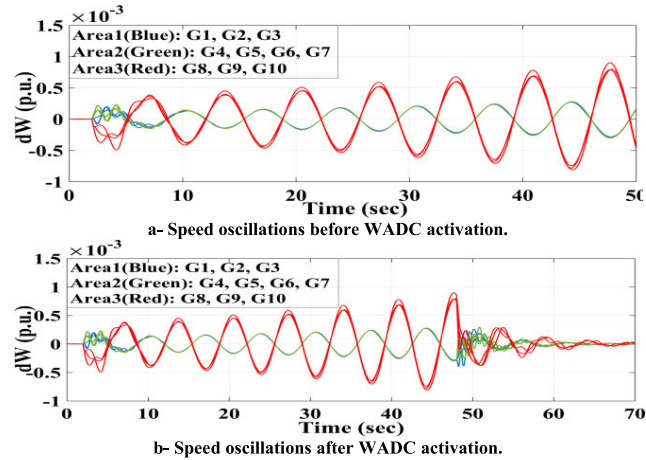


FIGURE 11. IAOs with and without WADC-Case 2.

inter-area speed deviations by activating the proposed WADC scheme are presented in Figure 9.

From Figure 9, it is shown that by implementing GCSs as input to the generators excitation systems, the corresponding IAOs damped properly with high damping ratio. Also, in order to evaluate the WADC damping performances against GIS time latencies, an additional simulation study is investigated. For this issue, considering 0.2 second time latency, it is considered that the evaluated GISs are transmitted through communication channels with unavoidable 0.2 second time latency. The proposed WADC damping performance in the presence of communication time delay is shown in in Figure 10.

As it can be seen, however, there are some weaknesses through damping performances, but the proposed WADC scheme represents positive performances which the main speed deviations through two oscillating areas are damped properly within short time durations.

2) CASE 2

In the second scenario, by changing the system topological and operational conditions, damping performance of proposed WADC scheme with respect to an unseen IAO is evaluated. For this issue, at the load level $LL=7223$ MW, a 3-phase short circuit event is occurred on line 15-16 at $t=2$ second. Considering the tie-line relay actions, two lines 15-16 and 2-3 are tripped at $t_1 = 2.1$ second and $t_2 = 2.4$ second,

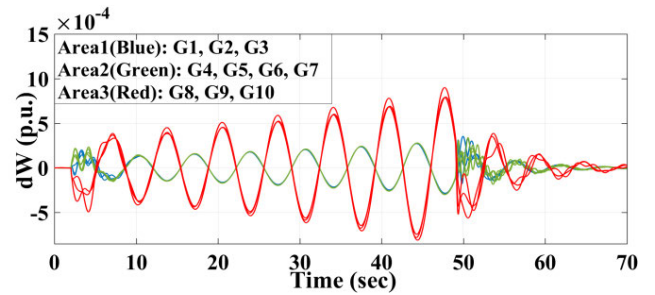


FIGURE 12. WADC damping performance in the presence of time delay-Case 2.

TABLE 3. Comparing proposed WADC results with respect to other schemes.

Ref.	Scenario 1			Scenario 2			Dynamic Stability
	ID11 (p.u.)	ID12 (p.u.)	IDI (p.u.)	ID (p.u.)	ID12 (p.u.)	IDI (p.u.)	
[2]	4.16	2.012	2.07	5.29	2.44	2.16	Stable
[8]	4.16	3.13	1.33	5.29	3.35	1.58	Stable
[12]	4.16	2.94	1.42	5.29	2.99	1.77	Stable
[33]	4.16	2.15	1.94	5.29	3.24	1.63	Stable
[34]	4.16	1.96	2.12	5.29	2.58	2.05	Stable
[35]	4.16	2.38	1.75	5.29	2.31	2.3	Stable
[19]	4.16	1.82	2.29	5.29	1.94	2.73	Stable
[36]	4.16	3.31	1.26	5.29	3.15	1.68	Stable
Proposed WADC	4.16	1.24	3.36	5.29	1.68	3.15	Stable

respectively. Speed deviations of the installed synchronous generators with respect to occurred fault event are presented in Figure 11-a. Considering the system dynamic behavior, generators oscillations are divided into two coherent groups as *Area1*(G1,G2,G3,G4,G5,G6,G7) and *Area2*(G8,G9,G10) which are oscillating against each other with the inter-area frequency $f = 0.131$ Hz. Based on the oscillating areas, GIS signals $\Delta\omega_{COI-1-2}$ and $\Delta\delta_{COI-1-2}$ are provided as input signals to CARTs which by passing 5 inter-area peak points, the controlling gains K_{1i} and K_{2i} are estimated. The controlling gains are estimated as $K_{1-CART1} = 57.19$ and $K_{2-CART2} = 42.29$ which are highly close with BGA evaluation results $K_{1-BGA} = 59.16$ and $K_{2-BGA} = 41.895$. Speed oscillations of the system synchronous generators after applying WADC scheme are illustrated in Figure 11-b. Similar to *Case-1*, by applying the proposed WADC scheme, the system dynamic oscillations are damped properly with high damping ratio.

Also, in the case of validating WADC scheme within communication channels time latencies, considering $t = 0.2$ second time delay through GIS signals, the WADC damping performances are evaluated and shown in Figure 12. As it can be seen, time delay has a few negative effects through damping performance, however, the proposed WADC scheme are able to damp the oscillations through short time durations.

C. COMPARISON OF THE PROPOSED WADC SCHEME WITH RESPECT TO PREVIOUS WORKS

In this section, in order to evaluate the proposed WADC scheme with other methods, considering a few other

approaches published recently [2], [8], [12], [32], [33], [34], [35], [19], [36], a comparison study between damping performance of the proposed WADC and developed methods are performed. In this case, considering the same fault event scenarios presented in Section B and evaluating the system dynamic oscillations through IDI index, effectiveness of the developed WADC damping performances at two different time windows are evaluated as follows:

$$\begin{aligned}
 IDI &= IDI1/IDI2 \\
 \text{where ; } IDI1 &= \left[\sum_{t_1=t_f^+}^{t_2=t_{WADC}^-} \Delta\omega_{COI-AB} \right] \\
 IDI2 &= \left[\sum_{t_3=t_{WADC}^+}^{t_4=t_{WADC}^++5 \text{ cycles}} \Delta\omega_{COI-AB} \right] \quad (22)
 \end{aligned}$$

where, $\Delta\omega_{COI-AB}^{\Delta t_1=t_f-t_{WADC}}$ and $\Delta\omega_{COI-AB}^{\Delta t_2=t_{WADC}^+-t_{5cycles}}$ are the inter-area speed deviations during five inter-area cycles before and after applying WADC schemes, respectively.

The system damping results for two inter-area fault event scenarios with respect to different WADC schemes are presented in Table 3.

From Table 3, it can be seen that through two provided fault scenarios, WADC techniques indicate different damping performances in evaluated IDI values. In this case, however all of provided approaches are able to control the inter-area oscillations, but the proposed WADC scheme present better efficiency with proper damping ratio comparing with other WADC techniques. The main advantage of the proposed WADC scheme is its lack of requirements to the system settings which can be used on wide variety of applications. Also, in comparison, most other techniques [12], [33], [35], [19], [36] highly depend on the system topological conditions which in the case of changing the system impedance matrixes, several updates are needed. However, based evaluated results based on WAMS technology, the proposed WADC scheme can be used on different power systems with lower costs and complexities.

VI. CONCLUSION

In this paper, a CART-based WADC scheme was proposed for damping IAO. For this propose, based on the WAMS technology through real-time working mode, the generators speed and rotor angle signals are estimated from which considering the correlation coefficients theory and using clustering technique, the oscillating area are identified. In the case of identifying unstable IAOs, the proposed WADC scheme is activated which proper GCSs with the aim of damping IAOs are provided. In this case, considering two adaptive CARTs into WADC scheme, the controlling gains K_1 and K_2 are estimated online which by multiplying the gains with GIS signals, proper GCSs are produced as input signals to generators excitation systems. The proposed WADC scheme has two offline and online working modes which first the optimal gain

estimators CART1 and CART2 are trained offline and then performed into real-time mode for online estimations of two individual controlling gains. Results indicate positive effects of the proposed WADC scheme for fast damping the IAOs with high damping ratio.

REFERENCES

- [1] M. J. Gibbard, *Small-Signal Stability, Control and Dynamic Performance of Power Systems*. Adelaide, SA, Australia: Univ. of Adelaide Press, 2015.
- [2] S. Ranjbar, M. Aghamohammadi, and F. Haghjoo, "A new scheme of WADC for damping inter-area oscillation based on CART technique and Thevenine impedance," *Int. J. Electr. Power Energy Syst.*, vol. 94, pp. 339–353, Jan. 2018.
- [3] J. Qi, Q. Wu, Y. Zhang, G. Weng, and D. Zhou, "Unified residue method for design of compact wide-area damping controller based on power system stabilizer," *J. Mod. Power Syst. Clean Energy*, vol. 8, no. 2, pp. 367–376, Mar. 2020.
- [4] Q. Mou, H. Ye, and Y. Liu, "Nonsmooth optimization-based WADC tuning in large delayed cyber-physical power system by interarea mode tracking and gradient sampling," *IEEE Trans. Power Syst.*, vol. 34, no. 1, pp. 668–679, Jan. 2019.
- [5] M. J. Alinezhad, M. Radmehr, and S. Ranjbar, "Adaptive wide area damping controller for damping inter-area oscillations considering high penetration of wind farms," *Int. Trans. Electr. Energy Syst.*, vol. 30, no. 6, Mar. 2020, Art. no. e12392.
- [6] J. Zhang, C. Y. Chung, C. Lu, K. Men, and L. Tu, "A novel adaptive wide area PSS based on output-only modal analysis," *IEEE Trans. Power Syst.*, vol. 30, no. 5, pp. 2633–2642, Sep. 2015.
- [7] M. E. C. Bento, "Fixed low-order wide-area damping controller considering time delays and power system operation uncertainties," *IEEE Trans. Power Syst.*, vol. 35, no. 5, pp. 3918–3926, Sep. 2020.
- [8] A. Thakallapelli and S. Kamalasadani, "Measurement-based wide-area damping of inter-area oscillations based on MIMO identification," *IET Gener., Transmiss. Distrib.*, vol. 14, no. 13, pp. 2464–2475, Jul. 2020.
- [9] D. D. Simfukwe, B. C. Pal, N. Martins, and R. A. Jabr, "Robust and low-order design of flexible AC transmission systems and power system stabilisers for oscillation damping," *IET Gener., Transmiss. Distrib.*, vol. 6, no. 5, pp. 445–452, May 2012.
- [10] M. Khaji and M. R. Aghamohammadi, "Emergency transmission line switching to suppress power system inter-area oscillation," *Int. J. Electr. Power Energy Syst.*, vol. 87, pp. 52–64, May 2017.
- [11] Y. Zhou, J. Liu, Y. Li, C. Gan, H. Li, and Y. Liu, "A gain scheduling wide-area damping controller for the efficient integration of photovoltaic plant," *IEEE Trans. Power Syst.*, vol. 34, no. 3, pp. 1703–1715, May 2019.
- [12] I. Zenelis, X. Wang, and I. Kamwa, "Online PMU-based wide-area damping control for multiple inter-area modes," *IEEE Trans. Smart Grid*, vol. 11, no. 6, pp. 5451–5461, Nov. 2020.
- [13] Y. Shen, W. Yao, J. Wen, H. He, and L. Jiang, "Resilient wide-area damping control using GrHDP to tolerate communication failures," *IEEE Trans. Smart Grid*, vol. 10, no. 3, pp. 2547–2557, May 2019.
- [14] N. R. Naguru and V. Sarkar, "Practical supplementary controller design for the bi-layer WAC architecture through structurally constrained H_2 norm optimisation," *IET Gener., Transmiss. Distrib.*, vol. 13, no. 7, pp. 1095–1103, Apr. 2019.
- [15] L. Simon, K. S. Swarup, and J. Ravishankar, "Wide area oscillation damping controller for DFIG using WAMS with delay compensation," *IET Renew. Power Gener.*, vol. 13, no. 1, pp. 128–137, Jan. 2019.
- [16] T. Amraee and S. Ranjbar, "Transient instability prediction using decision tree technique," *IEEE Trans. Power Syst.*, vol. 28, no. 3, pp. 3028–3037, Aug. 2013.
- [17] X. Shi, Y. Cao, M. Shahidehpour, Y. Li, X. Wu, and Z. Li, "Data-driven wide-area model-free adaptive damping control with communication delays for wind farm," *IEEE Trans. Smart Grid*, vol. 11, no. 6, pp. 5062–5071, Nov. 2020.
- [18] T. Surinkaew, R. Shah, M. Nadarajah, and S. M. Muyeen, "Forced oscillation damping controller for an interconnected power system," *IET Gener., Transmiss. Distrib.*, vol. 14, no. 2, pp. 339–347, Jan. 2020, doi: 10.1049/iet-gtd.2019.1115.

- [19] N. R. Naguru and Y. B. Ganapavaram, "Design of a limited state feedback wide-area power system damping controller without communication channels," *IEEE Access*, vol. 8, pp. 160931–160946, 2020, doi: [10.1109/ACCESS.2020.3021599](https://doi.org/10.1109/ACCESS.2020.3021599).
- [20] G. N. Baltas, N. B. Lai, L. Marin, A. Tarrasó, and P. Rodriguez, "Grid-forming power converters tuned through artificial intelligence to damp subsynchronous interactions in electrical grids," *IEEE Access*, vol. 8, pp. 93369–93379, 2020.
- [21] M. Sarkar, B. Subudhi, and S. Ghosh, "Unified Smith predictor based H_{∞} wide-area damping controller to improve the control resiliency to communication failure," *IEEE/CAA J. Autom. Sinica*, vol. 7, no. 2, pp. 584–596, Mar. 2020.
- [22] J. A. Oscullo and C. F. Gallardo, "Residue method evaluation for the location of PSS with sliding mode control and fuzzy for power electromechanical oscillation damping control," *IEEE Latin Amer. Trans.*, vol. 18, no. 1, pp. 24–31, Jan. 2020.
- [23] M. Rezaee, M. S. Moghadam, and S. Ranjbar, "Online estimation of power system separation as controlled islanding scheme in the presence of inter-area oscillations," *Sustain. Energy, Grids Netw.*, vol. 21, Mar. 2020, Art. no. 100306.
- [24] C. Li, Y. Sun, X. Chen, and Z. Ma, "Selection of global input signals for wide-area PSS to damp inter-area oscillations in multi-machine power systems," Presented at the Power Energy Eng. Conf. (APPEEC), Mar. 2010.
- [25] S. Ghosh, Y. J. Isbeih, M. S. El Moursi, and E. F. El-Saadany, "Cross-Gramian model reduction approach for tuning power system stabilizers in large power networks," *IEEE Trans. Power Syst.*, vol. 35, no. 3, pp. 1911–1922, May 2020.
- [26] T. Wang, A. Pal, J. S. Thorp, Z. Wang, J. Liu, and Y. Yang, "Multi-polytope-based adaptive robust damping control in power systems using CART," *IEEE Trans. Power Syst.*, vol. 30, no. 4, pp. 2063–2072, Jul. 2015.
- [27] L. Cheng, G. Chen, W. Gao, F. Zhang, and G. Li, "Adaptive time delay compensator (ATDC) design for wide-area power system stabilizer," *IEEE Trans. Smart Grid*, vol. 5, no. 6, pp. 2957–2966, Nov. 2014.
- [28] C. Sharma and B. Tyagi, "Fuzzy type-2 controller design for small-signal stability considering time latencies and uncertainties in PMU measurements," *IEEE Syst. J.*, vol. 11, no. 2, pp. 1149–1160, Jun. 2017.
- [29] I. Sephehrirad, R. Ebrahimi, E. Alibeiki, and S. Ranjbar, "Intelligent differential protection scheme for controlled islanding of microgrids based on decision tree technique," *J. Control, Autom. Electr. Syst.*, vol. 31, no. 5, pp. 1233–1250, Apr. 2020.
- [30] M. R. Aghamohammadi and S. M. Tabandeh, "A new approach for online coherency identification in power systems based on correlation characteristics of generators rotor oscillations," *Int. J. Electr. Power Energy Syst.*, vol. 83, pp. 470–484, Dec. 2016.
- [31] R. Shah, N. Mithulananthan, A. Sode-Yome, and Kwang. Y. Lee, "Impact of large-scale PV penetration on power system oscillatory stability," in *Proc. IEEE PES Gen. Meeting*, Minneapolis, MN, USA, Jul. 2010, pp. 1–7, doi: [10.1109/PES.2010.5589660](https://doi.org/10.1109/PES.2010.5589660).
- [32] S. You, G. Kou, Y. Liu, X. Zhang, Y. Cui, M. J. Till, W. Yao, and Y. Liu, "Impact of high PV penetration on the inter-area oscillations in the U.S. Eastern Interconnection," *IEEE Access*, vol. 5, pp. 4361–4369, 2017, doi: [10.1109/ACCESS.2017.2682260](https://doi.org/10.1109/ACCESS.2017.2682260).
- [33] E. Rebello, L. Vanfretti, and M. S. Almas, "Experimental testing of a real-time implementation of a PMU-based wide-area damping control system," *IEEE Access*, vol. 8, pp. 25800–25810, 2020, doi: [10.1109/ACCESS.2020.2970988](https://doi.org/10.1109/ACCESS.2020.2970988).
- [34] M. E. C. Bento, D. Dotta, R. Kuiuava, and R. A. Ramos, "A procedure to design fault-tolerant wide-area damping controllers," *IEEE Access*, vol. 6, pp. 23383–23405, 2018, doi: [10.1109/ACCESS.2018.2828609](https://doi.org/10.1109/ACCESS.2018.2828609).
- [35] A. Husham, A. E.-D. Hussein, M. A. Abido, and I. Kamwa, "Scattering transformation based wide-area damping controller of SSSC considering communication latency," *IEEE Access*, vol. 9, pp. 15510–15519, 2021, doi: [10.1109/ACCESS.2021.3052417](https://doi.org/10.1109/ACCESS.2021.3052417).
- [36] A. Sharafi, A. Vahidnia, M. Jalili, and G. Ledwich, "Adaptive wide-area control of power systems through dynamic load modulating SVCs," *IEEE Access*, vol. 10, pp. 22980–22996, 2022, doi: [10.1109/ACCESS.2022.3149801](https://doi.org/10.1109/ACCESS.2022.3149801).



SOHEIL RANJBAR was born in Nour, Iran, in 1985. He received the Ph.D. degree in electrical engineering from Shahid Beheshti University, Tehran, Iran, in 2018. He is currently an Assistant Professor with the Electrical Engineering Department, Velayat University, Iranshahr, Iran. His research interests include bulk and micro-grid power system performance, such as transient and low-frequency oscillations including damping inter-area oscillations and resilience schemes on power systems.

• • •